SLAC-PUB-971
(TH) and (EXP)
September 1971

THE REACTION $\gamma p \rightarrow \pi^+ \pi^- p$ AT 5.5 TO 18 GeV AND A DUAL RESONANCE MODEL*

Joseph C. H. Park†
Stanford Linear Accelerator Center
Stanford University, Stanford, California 94305

ABSTRACT

The reaction $\gamma p \rightarrow \pi^+ \pi^- p$ in the energy range 5.5 to 18 GeV has been studied in connection with the dual resonance model of Satz and Shilling. The data was obtained from streamer chamber exposures using an 18 GeV Bremsstrahlung beam. Some aspects of the data, such as the shape of ρ peak and the dependence of the diffraction slope on the dipion mass in the ρ region, are satisfactorily reproduced by the model. However, the model in their proposed form predicts a wrong energy dependence and disagrees badly with the observed ρ decay angular distributions.

(Submitted to Nuclear Physics.)

---

*Work supported by the U. S. Atomic Energy Commission.

†Now at Max-Planck-Institute fur Physik und Astrophysik, Munich, Germany.

The Veneziano models, explicitly satisfying duality and crossing symmetry, had considerable success in the phenomenology of non-diffractive processes.[1] Recently Satz et. al.[2,3] proposed a way of applying these ideas to the diffractive processes involving Pomeron exchange. In this report we compare their model with the data from the reaction

$$\gamma p \rightarrow \pi^+ \pi^- p \ , \qquad (1)$$

with the photon energy in the range, 5.5 to 18 GeV. Some aspects of the data, such as the shape of the ρ peak in the dipion mass spectrum and the dependence of the diffraction peak on the dipion mass in the ρ region, are satisfactorily reproduced by the model. However, the model in the proposed simple form predicts a wrong energy dependence and diagrees badly with the observed ρ decay angular distributions. The data, in this respect, strongly support the idea of s-channel helicity conservation[4,5] which appears incompatible with the model in study.[6]

The data used in the analysis was obtained in a photo-production experiment carried out at the Stanford Linear Accelerator Center exposing the 2-meter streamer chamber with a hydrogen gas target to an 18 GeV Bremsstrahlung beam.[7] Measurements of 21,000 3-prong events yielded 5800 events in the final state (1) at all photon energies. Some properties of ρ production in this data, such as the total and differential cross sections and decay angular characteristics have been described elsewhere.[8] For the present study we use a subsample consisting of 2800 events with the energy above 5.5 GeV. Each event is then weighted to correct for the trigger and chamber efficiency. These weights for high energy events behave mildly: the average weight for our sample is 1.5 and only a few events (about 7%) have weights larger than 2. The presence of the target tube ($\frac{1}{2}$ inch diameter, 4 mil thick mylar

tube) made the vertex region invisible. This caused a scanning bias in detecting very low energy protons and high energy forward pions (staying invisible for some distance away from the vertex). The effect is apparent in the data as a depletion of events with the momentum transfer near minimum. Extrapolating to the minimum by means of exponential fits such as in Table I (to be described later) we estimate the overall loss to be less than 10%.

The reaction (1) at high energy is well known to be completely dominated by the diffractive production of ρ[8,9]: The flat cross section as a function of the total energy, the similarity of the momentum transfer distribution to the πp diffraction scattering, and the evidence for the natural parity exchange from the polarized photon experiment[5] all support the idea that the reaction proceeds through Pomeron (P) exchange as in Fig. 1.

The model of Satz and Schilling. We briefly review the model of Satz and Schilling.[3] Using the notations of Fig. 1 we define the invariants, $\bar{s} = (k + p)^2$, $\bar{t} = (p_1 - p_2)^2$, $s = (q_1 + q_2)^2$, $t = (k - q_2)^2$, and $u = (k - q_2)^2$. The essential idea is to treat the Pomeron as a $J^P = 0^+$ particle and factorize the amplitude as

$$\mathcal{M}(\gamma p \to \pi^+\pi^- p) = \exp\left(\frac{a}{2}\,\bar{t}\right)\bar{s}\,\mathcal{M}(\gamma P \to \pi^+\pi^-), \tag{2}$$

where the first factor is the P-p-p vertex function, $\bar{s}$ is the Pomeron propagator, and the last factor stands for the amplitude of the two body process,

$$\gamma p \to \pi^+\pi^- \tag{3}$$

For the latter process A. Bartl and C. Iso[10] have pointed out that (treating P as a 0^+ particle) gauge invariance leads to the following kinematic factor

$$\mathcal{M}(\gamma P \to \pi^+\pi^-) = \left[(k\cdot Q\ \epsilon\cdot q - k\cdot q\ \epsilon\cdot Q)\ /\ k\cdot Q\right]\ V, \tag{4}$$

where $Q = q_1 + q_2$ and $q = q_1 - q_2$. Finally the B_4-prescription of Venenziano is applied to the amplitude V using the ρ and π trajectories in the direct and crossed channels respectively.

$$V = \beta\left[B(1 - \alpha_\rho(s)_1 - \alpha_\pi(t)) + B(1 - \alpha_\rho(s)_1 - \alpha_\pi(u))\right] . \qquad (5)$$

The trajectory functions are taken to be

$$\alpha_\pi(x) = \alpha'\left(x - m_\pi^2\right) , \qquad (6a)$$

$$\alpha_\rho(x) = 1 + \alpha'\left(x - m_\rho^2\right) + i\alpha'\left(x - 4m_\pi^2\right) \frac{m_\rho \Gamma_\rho}{\left(m_\rho^2 - 4m_\pi^2\right)} \theta\left(x - 4m_\pi^2\right) . \qquad (6b)$$

We use the prevalent values for the slopes of trajectories, $\alpha' = 1\ \mathrm{GeV}^{-2}$, the p-p diffraction slope, $a = 5\ \mathrm{GeV}^{-2}$, and the nominal values for ρ, $m_\rho = 765$ MeV and $\Gamma_\rho = 125$ MeV.

The model in this simple form has <u>no</u> free parameters other than the overall normalization (at a fixed energy) β of Eq. (5). Combining Eqs. (2) - (5) we obtain the following expression for the cross section averaged over the photon polarization ϵ,

$$\partial\sigma = \frac{\pi}{k_{1ab} m_p} \partial\Phi_3 \exp(a\bar{t})\, \bar{s}^{\,2}\left(s - 4m_\pi^2\right) \sin^2\theta_J\, |V|^2 , \qquad (7)$$

where $\partial\Phi_3$ is the invariant 3-body phase space and θ_J is the decay angle in the t-channel helicity frame for the dipion system to be discussed later.

<u>Energy dependence</u>. The numerical results were obtained by a Monte-Carlo technique with the Bremsstrahlung shape, $1/k_{1ab}$, folded in. Also for the sake of efficiency the calculations were performed with the cuts, $m(\pi\pi) < 2$ Gev and

$|\bar{t}| < 0.8$ GeV^2. If β is taken to be independent of energy, then the model shows a rising energy depednence ($\propto \bar{s}^{1/2}$). In order to force an agreement with the data we had to introduce an ad hoc factor $\bar{s}^{-3/2}$ in the calculation. The energy dependence is shown in Fig. 2, in which we compare the observed photon energy spectrum with the calculated curve (normalized to the total number of events).

Invariant mass and momentum transfer distributions. In Figs. 3 and 4 we show two-body invariant mass distributions together with the calculated curves. Neither of the two pion-nucleon mass spectra of Fig.-3 exhibits any prominent structures (such as $\Delta(1236)$ for the $m(p\pi^+)$ spectrum). The gross shapes of the two distributions are similar, which is consistent with a model with $t \longleftrightarrow u$ (or $\pi^+ \longleftrightarrow \pi^-$) symmetry. The results of calculations are obtained as distributions such as that shown by dots in the $m(p\pi^-)$ spectrum of Fig. 3; smooth curves in this and other figures are free-hand representations of such distributions. As shown in Fig. 3 the model does not agree well with the data; this reflects, of course, the disagreement in the dipion decay angular distributions to be discussed later.

Fig. 4 shows the $m(\pi\pi)$ spectrum which is dominated by ρ. Here the model satisfactorily reproduces the ρ shape; both features, namely, the shift of the peak from the nominal value (765 MeV) to the observed one (750 MeV) and the skewing of the resonance shape are well reproduced. However, outside the ρ region, $1 < m(\pi\pi) < 2$ GeV, the model exhibits two characteristic oscillations which the data do not seem to warrant. Also in this mass region the predicted cross section is larger than observed by a factor two.

Fig. 5 is the proton-proton momentum transfer ($\bar{t}$) distribution for all events. In order to remove the kinematic variation of minimum $\bar{t}$ on the

photon energy we consider the quantity

$$\bar{t}' = \bar{t} - \bar{t}_{min} = -2k^* p_2^* (1 - \cos\theta^*) \quad , \tag{8}$$

where $k^*(p_2^*)$ is the momentum of γ (outgoing proton) and θ^* is the production angle of the dipion system in the overall center-of-mass. There is a satisfactory agreement between the data and the calculation disregarding the dip in the first bin ($|\bar{t}'| < 0.02$ GeV^2), which is due to a bias in the data as mentioned earlier.

In Figs. 6 and 7 we show a peculiar feature, which appears to be characteristic of the diffraction dissociation process,[11] namely, the dependence of the diffraction peak on the dipion mass. The $\bar{t}$ distributions in several $m(\pi\pi)$ intervals together with the corresponding calculated curves are presented in Fig. 6. We also make an exponential fit of the form

$$A \exp(b\bar{t}') \tag{9}$$

for $0.02 < |\bar{t}'| < 0.52$ GeV^2 to each of these distributions and show in Fig. 7 the variation of the slope b as a function of $m(\pi\pi)$. The results are also listed in Table I. As seen in Fig. 7 the slope b of the data decreases monotonically from a value of 9.3 to 4.5 GeV^{-2} as the mass $m(\pi\pi)$ increases from a value of 0.48 to 0.96 GeV. In the same mass region the model also predicts a similar feature as shown by the smooth curve in the figure, but the predicted rise for higher mass appears inconsistent with the data.

Decay angular distributions. When considering the dipion decay angular distributions, the model tends to agree better with the data for high mass and disagrees badly in the ρ region. This is in contrast to the dipion mass and the

diffraction peak.

In the rest frame of the dipion system we introduce two sets of coordinate systems; (1) the t-channel helicity or Jackson axes defined as $\hat{z} = \hat{k}$, $\hat{y} = -\hat{k} \times \hat{p}_2 / |\hat{k} \times \hat{p}_2|$, $\hat{x} = \hat{y} \times \hat{z}$; and (2) the s-channel helicity axes, $\hat{z}_H = -\hat{p}_2$, $\hat{y}_H = \hat{y}$, $\hat{x}_H = \hat{y}_H \times \hat{z}_H$. The two systems are related to each other by a rotation through an angle χ about the common y-axis.[12] We then consider the polar and azimuth angles of $\hat{q}_1(\pi^+)$ in each coordinate systems,

$$\cos\theta_J = \hat{q}_1 \cdot \hat{z} \ , \quad \phi_J = \tan^{-1}(\hat{q}_1 \cdot \hat{y} \ / \ \hat{q}_1 \cdot \hat{x}), \tag{10a}$$

$$\cos\theta_H = \hat{q}_1 \cdot \hat{z}_H \ , \quad \phi_H = \tan^{-1}(\hat{q}_1 \cdot \hat{y}_H / \hat{q}_1 \cdot \hat{x}_H). \tag{10b}$$

For a parity-conserving decay, $1^- \rightarrow 0^-0^-$, (with the choice of y-axis normal to the production plane as in both systems) we expect the following general expression for the angular distribution,[13]

$$\frac{\partial W}{\partial \Omega} = \frac{3}{4\pi}\left[\rho_{00}\cos^2\theta + \rho_{11}\sin^2\theta - \rho_{1-1}\sin^2\theta\cos^2\phi - \sqrt{2}\,(\mathrm{Re}\,\rho_{10})\sin^2\theta\cos\phi\right], \tag{11}$$

$$= \frac{1}{\sqrt{4\pi}}\left[Y_{00} + (1 - 3\rho_{11})\frac{2}{\sqrt{5}}Y_{20} - \rho_{1-1}\sqrt{\frac{24}{5}}(\mathrm{Re}\,Y_{22}) + (\mathrm{Re}\,\rho_{10})\sqrt{\frac{48}{5}}(\mathrm{Re}\,Y_{21})\right]. \tag{12}$$

So that the density matrix elements are related to the multipole moments as given below

$$\rho_{11} = \frac{1}{3} - \frac{\sqrt{5}}{6}\langle Y_{20} / Y_{00}\rangle, \tag{13}$$

$$\rho_{1-1} = -\sqrt{\frac{5}{6}}\ \mathrm{Re}\langle Y_{21} / Y_{00}\rangle .$$

$$\mathrm{Re}\,\rho_{10} = \sqrt{\frac{5}{12}}\ \mathrm{Re}\langle Y_{21} / Y_{00}\rangle .$$

Since the t $\longleftrightarrow$ u crossing corresponds to a change of sign in $\cos\theta_J$, it is obvious from Eqs. (5) and (7) that the model is an even function of $\cos\theta_J$. Also it is a constant in ϕ_J. Furthermore we expect from the model that the projected $\cos\theta_H$ distribution is symmetric about 0 and the projected ϕ_H distribution is symmetric and invariant under $\phi_H \rightarrow \phi_H + \pi$.

In Fig. 8 we show the projected angular distributions. The $\cos\theta_H$ or ϕ_J distribution clearly shows the overall disagreement between the model and the data. In Figs. 9 and 10 we display the data and the calculation in several $m(\pi\pi)$ slices.

In each of the $m(\pi\pi)$ slices we have carried out a moment analysis and expressed the observed moments in terms of a density matrix assuming $J^P = 1^-$, according to Eq. (13). The results are summarized in Table II. The corresponding projections are given as dashed curves in Figs. 9 and 10 and show to what extent the observed angular distributions are consistent with the assignment, $J^P = 1^-$.

We observe that in the ρ region (the third and fourth mass intervals) the data is completely characterized by a vector meson decay with the polarization expected from the s-channel helicity conservation, namely $\rho^H_{11} = \frac{1}{2}$, $\rho^H_{01} = \rho^H_{1-1} = 0$ (as opposed to the case of the t-channel helicity non-flip, $\rho^J_{11} = \frac{1}{2}$, $\rho^J_{01} = \rho^J_{1-1} = 0$). The angular distribution in the s-channel helicity system is simply

$$\frac{\partial W}{\partial \Omega_H} = \frac{3}{8\pi} \sin^2\theta_H \ . \qquad (14)$$

We propose another test for $J^P = 1^-$ and s-channel helicity conservation. Assuming $J^P = 1^-$ and rotating through an angle χ about the y-axis[15] we obtain from Eq. (14) the following expression for the angular distribution in the t-channel

helicity or Jackson frame,

$$\frac{\partial W}{\partial \Omega_J} = \frac{3}{8\pi}\left[\frac{2}{3}+\left(\frac{1}{3}-\langle\cos^2\chi\rangle\right)\left(-\frac{1}{2}+\frac{3}{2}\cos^2\theta_J\right. - \frac{1}{2}\langle\sin^2\chi\rangle \sin^2\theta_J\cos^2\phi_J \qquad (15)$$

$$\left. + \langle\sin\chi\cos\chi\rangle\sin^2\theta_J\cos\phi_J\right].$$

Thus for a vector meson decay s-channel helicity conservation implies in the t-channel helicity frame

$$\rho^J_{11} = \frac{1}{4}\ (1 + \langle\cos^2\chi\rangle),$$

$$\rho^J_{1-1} = \frac{1}{4}\langle\sin^2\chi\rangle, \qquad (16)$$

$$\text{Re}\ \rho^J_{01} = \frac{1}{\sqrt{8}}\langle\sin\chi\cos\chi\rangle.$$

We observe in the data of the third (and fourth) mass region $\langle\cos^2\chi\rangle = 0.41\ (0.43)$ and $\langle\sin\chi\cos\chi\rangle = 0.37\ (0.38)$. Hence from Eq. (16) we obtain $\rho^J_{11} = 0.35\ (0.36)$, $\rho^J_{1-1} = 0.15\ (0.12)$, and Re $\rho_{01} = 0.13\ (0.13)$. Comparing these values with the corresponding values in Table II as a test for the s-channel helicity conservation (and the extent to which the data is dominated by $J^P = 1^-$) in the t-channel helicity frame we find good agreement. In addition the obvious relation, $\rho^J_{11} + \rho^J_{1-1} = \frac{1}{2}$ (independent of χ), is well satisfied by the data in the ρ region. All of this evidence confirm that in the mass region, $0.64 < m(\pi\pi) < 0.80$ GeV, the data correspond to a pure ρ decay, which is produced conserving the s-channel helicity. As is apparent in Figs. 9 and 10, particularly in the $\cos\theta_H$ and ϕ_J distributions, the model is incompatible with these features of the data.

In the higher mass regions outside the ρ, however, the model shows improved

agreement with the data (apart from the normalization). For example, in the two highest mass regions in Fig. 10 the cos θ_J distributions exhibit a tendency to peak near cos $\theta_J = \pm 1$ and the ϕ_J distributions tend to be flat as predicted by the model. If we insist on the predominance of the $J^P = 1^-$ component in these mass regions, then we obtain the density matrix elements as given in Table II, and the dashed curves in Figs. 9 and 10. In particular in the region, $1.04 < m(\pi\pi) < 1.4$ GeV, the observed angular distributions appear consistent with a vector meson decay. However the density matrix elements (Table II) are much different from those in the ρ region implying a different production mechanism. In the highest mass interval studied, $1.4 < m(\pi\pi) < 2$ GeV, the data is <u>not</u> consistent with a dominant $J^P = 1^-$; the singular behavior of cos θ_J distribution near the edges, for example, as compared with the dashed curve in Fig. 9, indicates presence of partial wave component higher than $\ell = 1$.

We summarize by noting that the model of Satz and Schilling as applied to the reaction (1) with a wide energy range correctly describes the shape of ρ in the dipion mass spectrum and explains the mass dependence of the slope of the momentum transfer distribution in the ρ region. This is after the rising energy-dependence has been adjusted by an ad hoc factor. The decay angular distributions, when analyzed in several dipion mass slices, were found to be consistent with the assumption of a dominant vector meson decay up to the mass of 1.4 GeV. In particular the polarization in the ρ region is strongly characterized by the s-channel helicity conservation, which is incompatible with the model studied.

We wish to thank the members of the SLAC Streamer Chamber Group, M. Davier, I. Derado, D. C. Fries, F. F. Liu, R. F. Mozley, A. C. Odian, W. P. Swanson, F. Villa and D. E. Yount for the use of the data and helpful discussions.

REFERENCES

1. N. F. Bali, "Multiperipheral Models: Phenomenology," invited talk, International Conference on Particle Reactions at the New Accelerators, Madison, Wisconsin, March 1970; H. Satz, "An Introduction to Dual Resonance Models in Multiparticle Physics," lectures given at the Heidelberg-Karlsruhe Summer Institute in Theoretical Physics, July 1970 (To be published in Springer Tracts in Modern Physics.)
2. S. Pokorski and H. Satz, Nucl. Phys. B19, 113 (1970).
3. H. Satz and K. Schilling, Nuovo Cimento, 67A, 511 (1970).
4. F. J. Gilman et al., Phys. Letters 31B, 387 (1970).
5. J. Ballam et al., Phys. Rev. Letters 24, 960 (1970).
6. H. Satz and K. Schilling, Duality versus s Channel Helicity Conservation in Diffraction Dissociation, Ref. Th. 1252 CERN, 1970.
7. This is the second photoproduction experiment using the streamer chamber at SLAC. The experimental technique was similar to the first one which has been described in M. Davier et al., Phys. Rev. D1, 790 (1970). A detailed report on the experimental arrangement and the data analysis of the present experiment is in preparation.
8. J. Park et al., "The Reaction $\gamma p \rightarrow \rho^{o} p$ at 5.5 to 18 GeV, a preliminary report submitted to the International Symposium on Electron and Photon Interactions at High Energies (1971), Ithaca, N. Y. A final report is in preparation.

9. See, for instance, review talk by A. Silverman, Proceedings of the International Symposium on Electron and Photon Interactions at High Energies, Liverpool, England, Sept. 1969, edited by D. W. Braben, Daresbury Nuclear Physics Laboratory, Daresbury England, 1970; Separate reviews by G. Kramer and R. Marshall, Vector Meson Production and Omega-Rho Interference, Proceedings of the Daresbury Study Weekend, 12-14 June, 1970, edited by A. Donachie and E. Gabathuler, Daresbury Nuclear Physics Laboratory.

10. A. Bartl and C. Iso, On a Dual Model for Diffractive Two-Pion Electroproduction, Desy report 70/56, 1970.

11. H. Satz, Phys. Letters 32B , 380 (1970).

12. The angle χ is a function of s, $\bar{t}$, and $\bar{s}$. An explicit expression may be obtained by noting $\cos\chi = \hat{p}_2 \cdot \hat{z}$, $\sin\chi = \hat{p}_2 \cdot \hat{x}$ in the dipion rest-frame.

13. For general formalism see for instance the lecture by J. D. Jackson in High Energy Physics, edited by C. DeWitt and M. Jacob, Gordon and Breach Science Publishers Inc., New York, 1966.

14. The multipole moments are calculated as $\langle Y_{LM} \rangle = \sum_i w_i Y_{LM}(\Omega) \Big/ \sum_i w_i$ where w_i is the weight of the ith event. The errors are estimated as $\delta \langle Y_{LM} \rangle = \left[\sum w_i Y_{LM}^2 - \left(\sum w_i Y_{LM} \right)^2 \Big/ \sum w_i \right]^{1/2} \Big/ \sum w_i$.

15. Eq. (16) is easily obtained by noting $\rho^J_{mn} = \sum D^{(1)*}_{ma}(0, \chi, 0) \rho^H_{ab} D^{(1)}_{bn}(0, \chi, 0)$. Or in terms of Y_{LM} which transforms irreducibly. Most straightforward is to substitute $\cos\theta_H = -\sin\chi \sin\theta_J \cos\phi_J + \cos\chi \cos\theta_J$ in Eq. (14) to obtain Eq. (15) and compare with Eq. (12) to obtain ρ_{mn} .

Table I. Exponential Fit for $\bar{t}'$ in $0.02 < -\bar{t}' < 0.52$ GeV^2

$m(\pi\pi)$ interval (GeV)	Number of events[a] (data)	Number of events (fitted)	b (GeV^{-2})
0.40 - 0.56	249.0	263.1	9.29 ± 0.71
0.56 - 0.64	298.6	318.0	8.07 ± 0.59
0.64 - 0.72	619.3	664.6	7.90 ± 0.40
0.72 - 0.80	877.8	932.3	6.47 ± 0.30
0.80 - 0.88	383.7	402.5	5.05 ± 0.42
0.88 - 1.04	172.4	185.7	4.52 ± 0.60
1.04 - 1.40	96.1	99.3	4.23 ± 0.81
1.40 - 2.00	118.9	110.1	4.09 ± 0.73

a. For $0 < -\bar{t}' < 0.52$ GeV^2. The difference between the data and the fitted values is due to the bias in the data for $-\bar{t}' < 0.02$ GeV^2.

Table II. Decay Moment Analysis and Density Matrix Elements assuming $J^P = 1^-$

$m(\pi\pi)$ interval (GeV)	Number of events[a]	Moments observed in S-channel Helicity System[b] $\langle Y_{20}/Y_{00}\rangle$	$\mathrm{Re}\langle Y_{22}/Y_{00}\rangle$	$\mathrm{Re}\langle Y_{21}/Y_{00}\rangle$	Density Matrix Elements ρ^H_{11}	ρ^H_{1-1}	$\mathrm{Re}\rho^H_{01}$
0.40 - 0.56	262.7	-0.461 ± 0.047	-0.009 ± 0.051	-0.128 ± 0.038	0.505 ± 0.018	0.078 ± 0.047	-0.083 ± 0.025
0.56 - 0.64	307.2	-0.390 ± 0.042	-0.007 ± 0.044	-0.097 ± 0.037	0.479 ± 0.016	0.067 ± 0.040	-0.063 ± 0.024
0.64 - 0.72	631.3	-0.475 ± 0.027	-0.001 ± 0.031	0.004 ± 0.026	0.510 ± 0.010	0.001 ± 0.028	0.002 ± 0.017
0.72 - 0.80	903.9	-0.440 ± 0.024	0.005 ± 0.027	0.037 ± 0.022	0.497 ± 0.009	-0.005 ± 0.024	0.024 ± 0.014
0.80 - 0.88	405.7	-0.385 ± 0.039	0.009 ± 0.039	0.112 ± 0.033	0.444 ± 0.015	-0.008 ± 0.036	0.072 ± 0.021
0.88 - 1.04	188.5	-0.313 ± 0.060	-0.005 ± 0.056	0.233 ± 0.045	0.449 ± 0.022	+0.005 ± 0.052	0.145 ± 0.029
1.04 - 1.40	126.4	0.178 ± 0.090	0.005 ± 0.059	0.373 ± 0.056	0.270 ± 0.034	-0.005 ± 0.054	0.240 ± 0.036
1.40 - 2.00	176.6	0.480 ± 0.085	0.026 ± 0.048	0.445 ± 0.052	0.154 ± 0.032	-0.024 ± 0.044	0.287 ± 0.034

$m(\pi\pi)$ interval (GeV)	Number of events[a]	Moments observed in t-channel Helicity System $\langle Y_{20}/Y_{00}\rangle$	$\mathrm{Re}\langle Y_{22}/Y_{00}\rangle$	$\mathrm{Re}\langle Y_{21}/Y_{00}\rangle$	ρ^J_{11}	ρ^J_{1-1}	$\mathrm{Re}\rho^J_{01}$
0.40 - 0.56	262.7	-0.198 ± 0.058	-0.192 ± 0.047	0.153 ± 0.038	0.407 ± 0.021	0.175 ± 0.043	0.098 ± 0.025
0.56 - 0.64	307.2	-0.151 ± 0.052	-0.171 ± 0.042	0.154 ± 0.033	0.389 ± 0.019	0.156 ± 0.038	0.099 ± 0.022
0.64 - 0.72	631.3	-0.029 ± 0.039	-0.192 ± 0.027	0.232 ± 0.023	0.344 ± 0.015	0.175 ± 0.025	0.150 ± 0.015
0.72 - 0.80	903.9	-0.000 ± 0.033	-0.132 ± 0.023	0.215 ± 0.021	0.333 ± 0.012	0.121 ± 0.021	0.139 ± 0.013
0.80 - 0.88	405.7	0.166 ± 0.051	-0.133 ± 0.032	0.211 ± 0.033	0.271 ± 0.019	0.122 ± 0.029	0.136 ± 0.021
0.88 - 1.04	188.5	0.162 ± 0.078	-0.236 ± 0.047	0.030 ± 0.044	0.273 ± 0.029	0.216 ± 0.043	0.020 ± 0.028
1.04 - 1.40	126.4	0.515 ± 0.097	-0.090 ± 0.050	-0.194 ± 0.058	0.141 ± 0.036	0.082 ± 0.045	-0.125 ± 0.037
1.40 - 2.00	176.6	1.000 ± 0.084	0.029 ± 0.037	-0.144 ± 0.051	-0.039 ± 0.031	-0.026 ± 0.033	-0.093 ± 0.033

a. weighted by the trigger and chamber efficiency as explained in the text.

b. Moments and errors are obtained as described in Ref. 10.

1955B12

FIGURE CAPTIONS

1. Diagram for the diffractive reaction $\gamma p \rightarrow \pi^+ \pi^- p$.
2. Photon energy spectrum. Curve shows the energy dependence of the model multiplied by Bremsstrahlung shape $(1/k_{1ab})$ and an arbitrary factor $\bar{s}^{-3/2}$.
3. Pion-nucleon invariant mass distributions. Dots in the $m(p\pi^-)$ spectrum represent the result of the Monte-Carlo calculation of the model. Smooth curves here and in other figures are free-hand sketches of such distributions.
4. Dipion mass distribution. 6% (not shown) of the total events have $m(\pi\pi) > 2$ GeV.
5. Proton-proton momentum transfer distribution as defined by Eq. (8) in the text.
6. Proton-proton momentum transfer distributions in several $m(\pi\pi)$ intervals.
7. Slope of the diffraction peak as a function of $m(\pi\pi)$. The solid curve is the prediction of the model.
8. Decay angular distributions of dipion system for all events. Subscript H (J) refers to s-channel helicity (t-channel) helicity frame.
9. Angular distributions in the s-channel helicity frame in different $m(\pi\pi)$ intervals. The intervals are defined in Table II. Solid curves are predictions of the model. Dashed curves result if the dipion system has a unique $J^P = 1^-$ as discussed in the text.
10. Angular distributions in the t-channel helicity frame in different $m(\pi\pi)$ intervals. See caption for Fig. 9 for additional remarks.

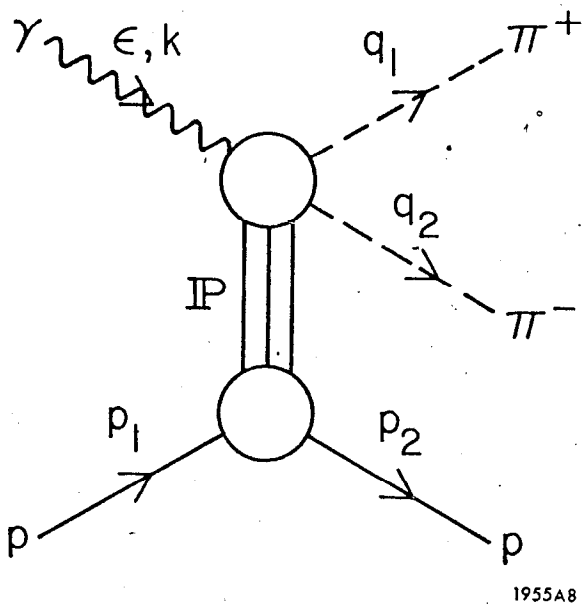

Fig. 1

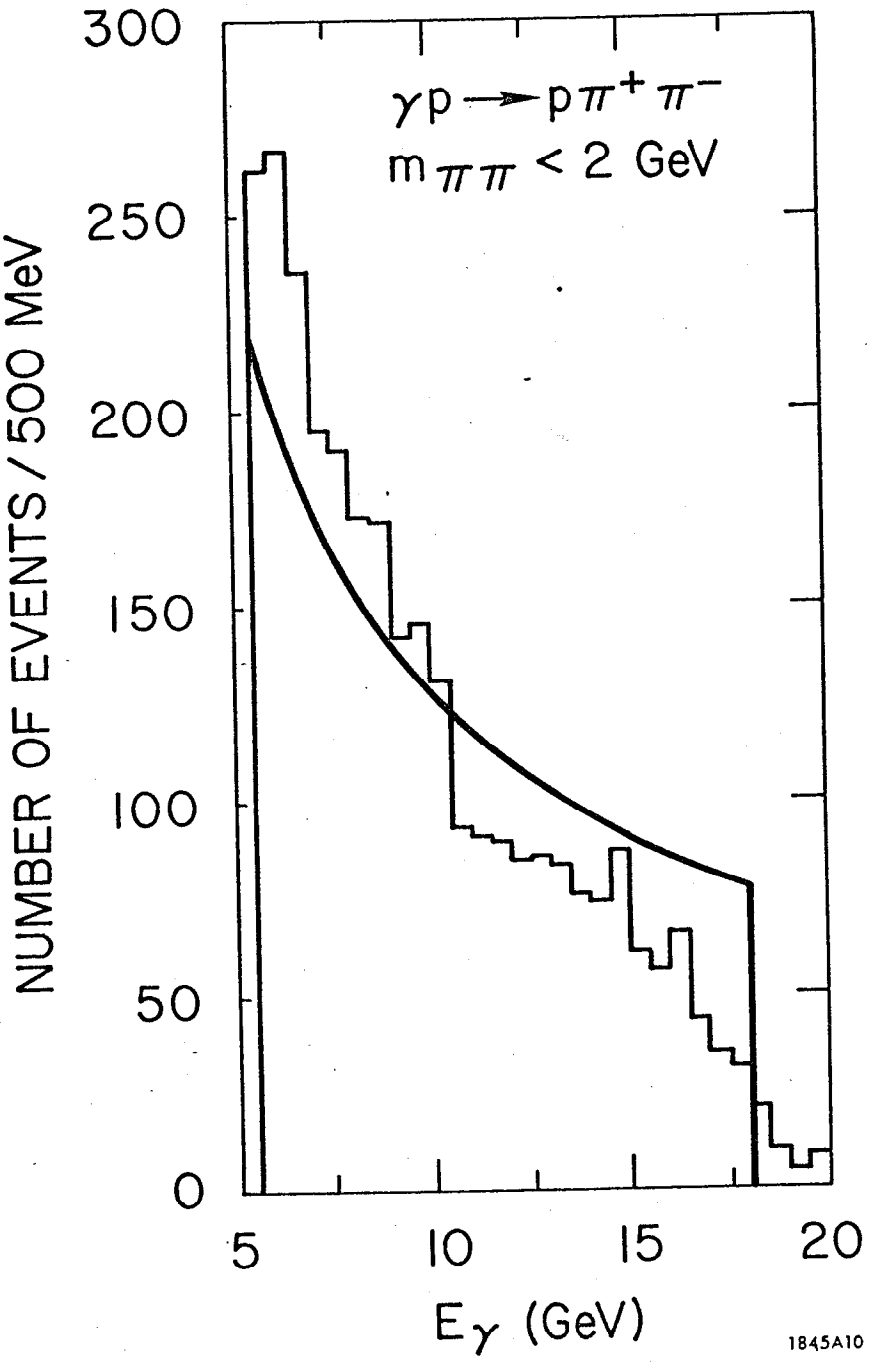
300
250
200
150
100
50
0
NUMBER OF EVENTS / 500 MeV
$\gamma p \rightarrow p\pi^+\pi^-$
$m_{\pi\pi} < 2$ GeV
5
10
15
20
E_γ (GeV)
1845A10

Fig. 2

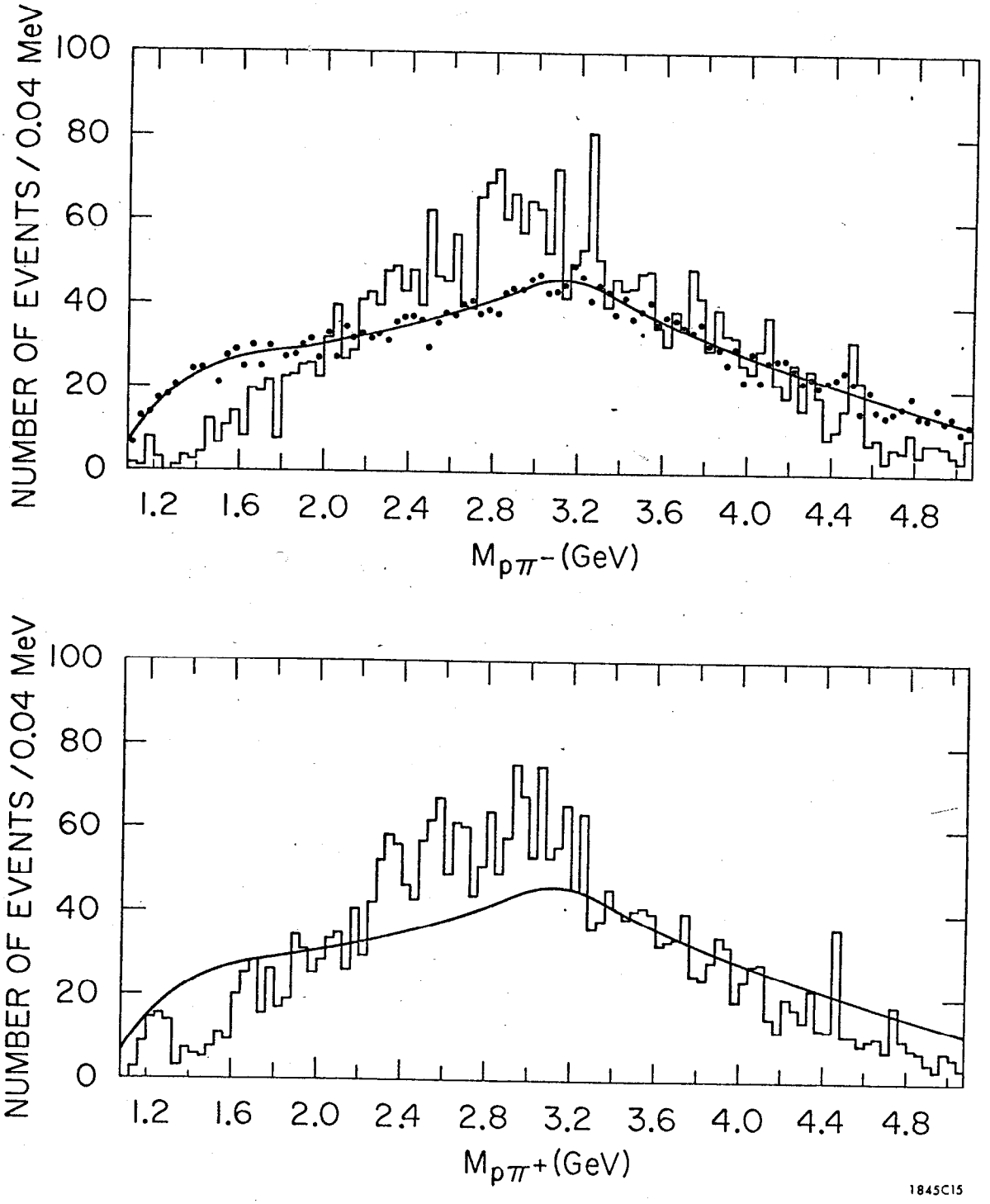
NUMBER OF EVENTS / 0.04 MeV
100
80
60
40
20
0
1.2
1.6
2.0
2.4
2.8
3.2
3.6
4.0
4.4
4.8
$M_{p\pi^-}$ (GeV)
NUMBER OF EVENTS / 0.04 MeV
100
80
60
40
20
0
1.2
1.6
2.0
2.4
2.8
3.2
3.6
4.0
4.4
4.8
$M_{p\pi^+}$ (GeV)
1845C15

Fig. 3

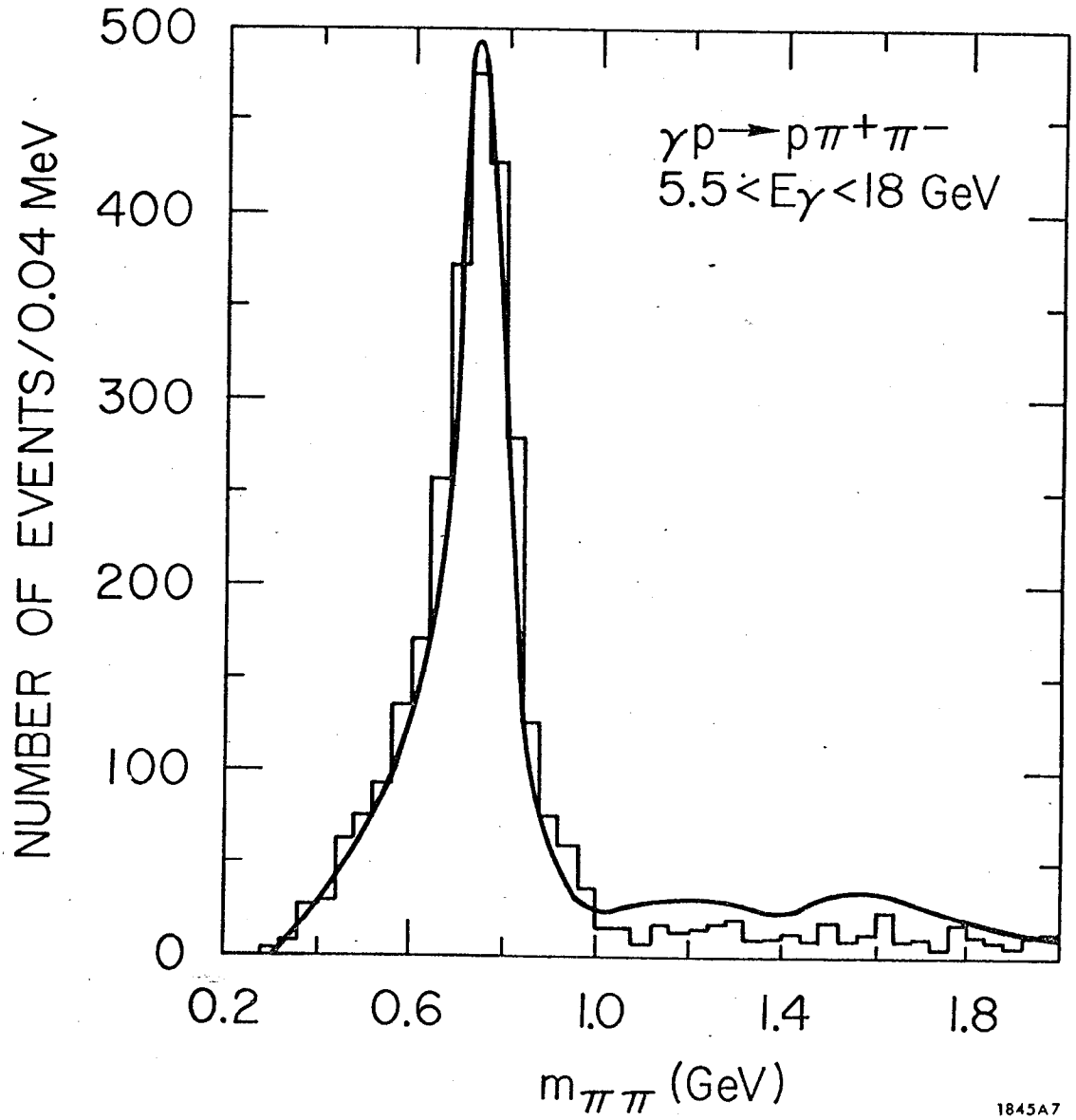
500
400
300
200
100
0
NUMBER OF EVENTS/0.04 MeV
γp→pπ+π−
5.5<Eγ<18 GeV
0.2
0.6
1.0
1.4
1.8
mππ (GeV)
1845A7

Fig. 4

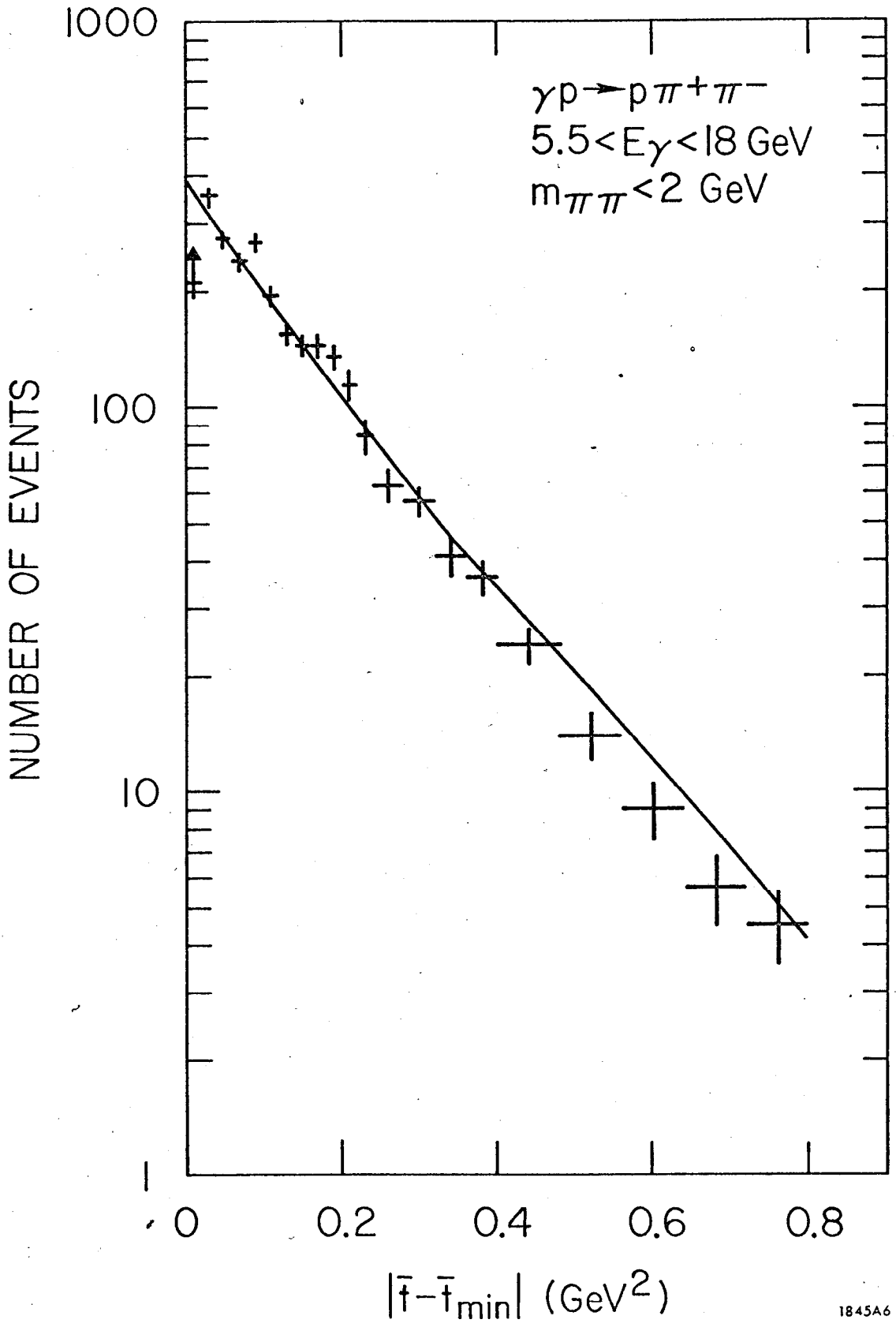
1000
100
10
1
NUMBER OF EVENTS
γp→pπ+π−
5.5<Eγ<18 GeV
mππ<2 GeV
0
0.2
0.4
0.6
0.8
|t̄−t̄min| (GeV²)
1845A6

Fig. 5

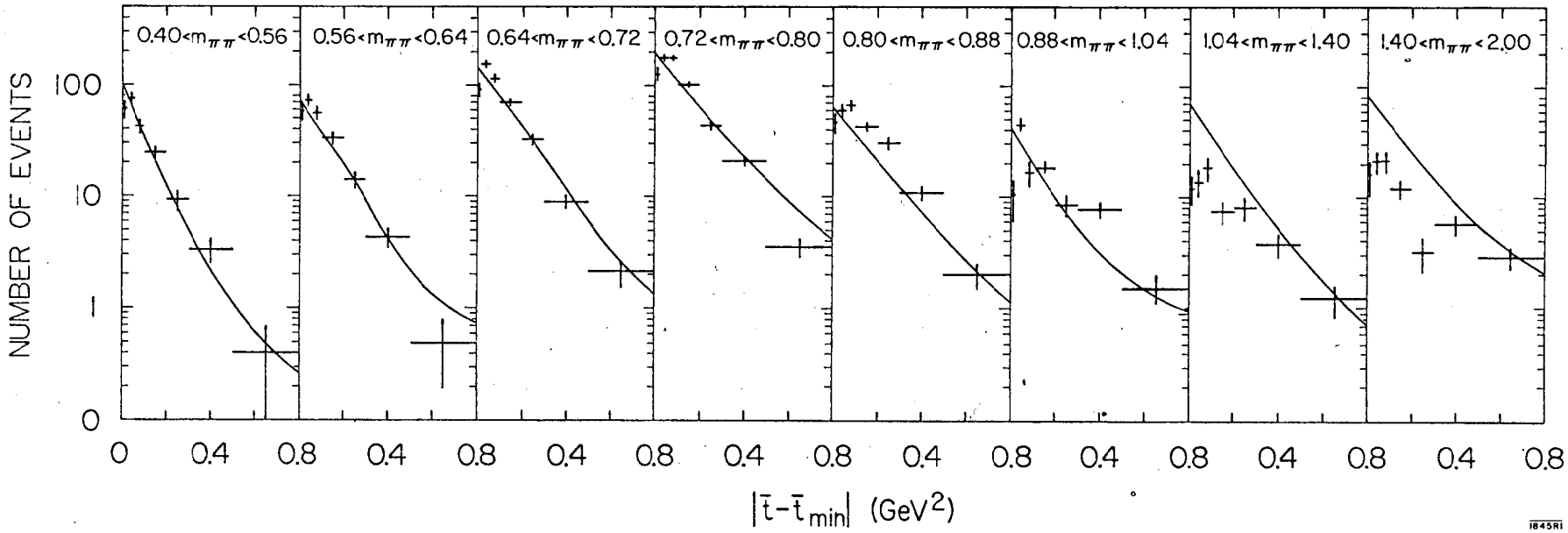
0.40<m$_{\pi\pi}$<0.56
0.56<m$_{\pi\pi}$<0.64
0.64<m$_{\pi\pi}$<0.72
0.72<m$_{\pi\pi}$<0.80
0.80<m$_{\pi\pi}$<0.88
0.88<m$_{\pi\pi}$<1.04
1.04<m$_{\pi\pi}$<1.40
1.40<m$_{\pi\pi}$<2.00
NUMBER OF EVENTS
100
10
1
0
0
0.4
0.8
$|\bar{t}-\bar{t}_{min}|$ (GeV^2)
1645R1

Fig. 6

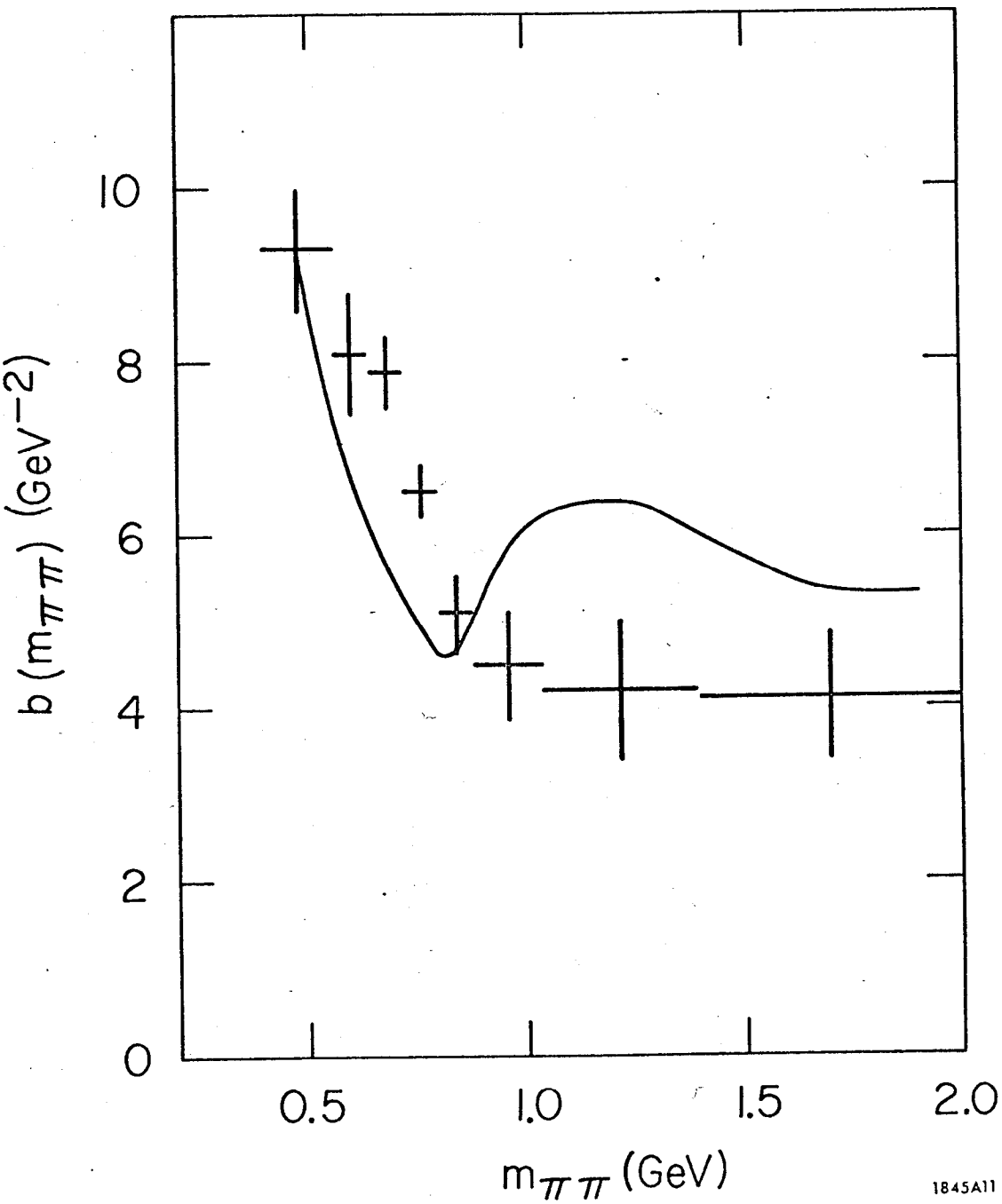

Fig. 7

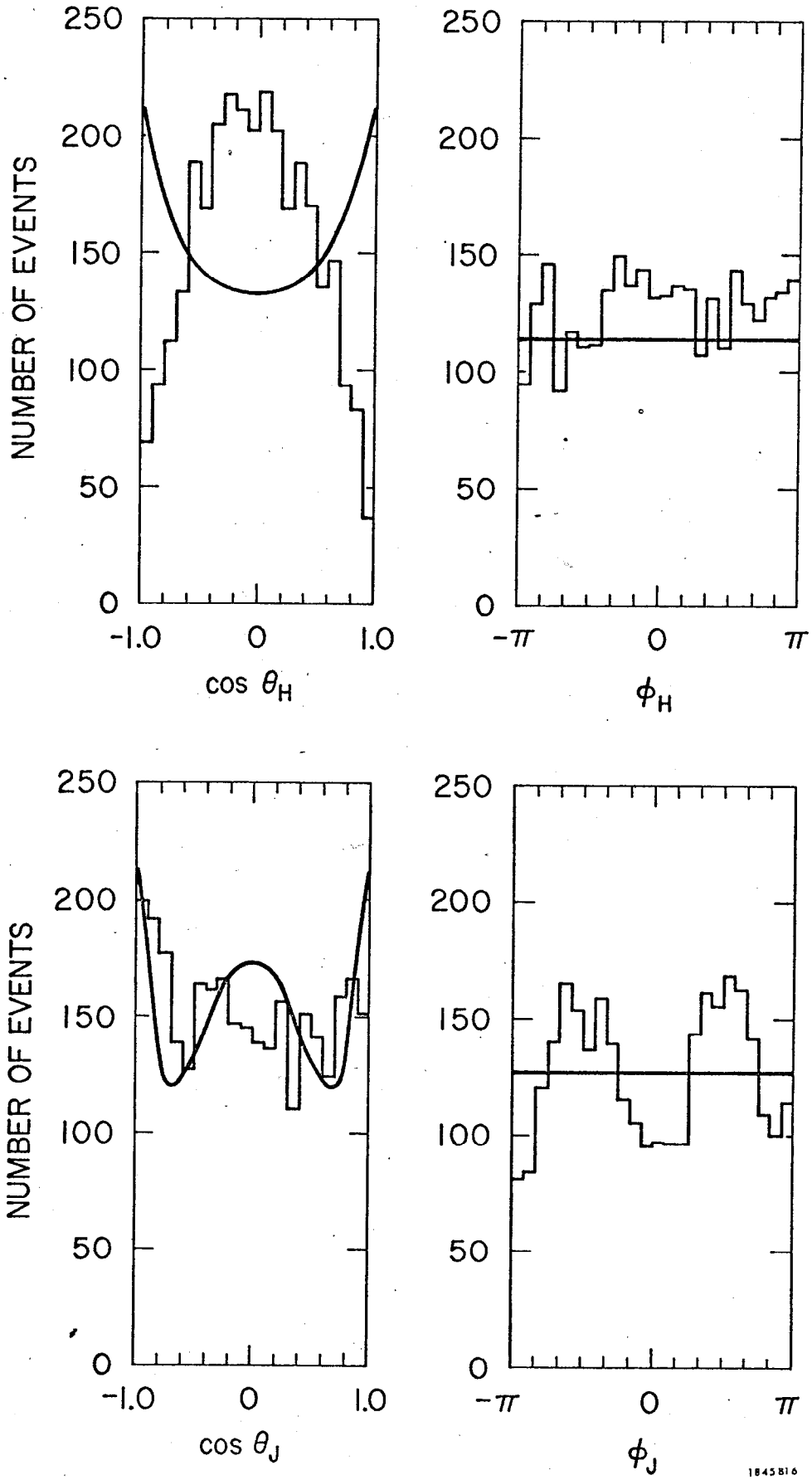
250
200
150
100
50
0
NUMBER OF EVENTS
-1.0
0
1.0
cos θ_H
$-\pi$
0
π
ϕ_H
cos θ_J
ϕ_J
1845816

Fig. 8

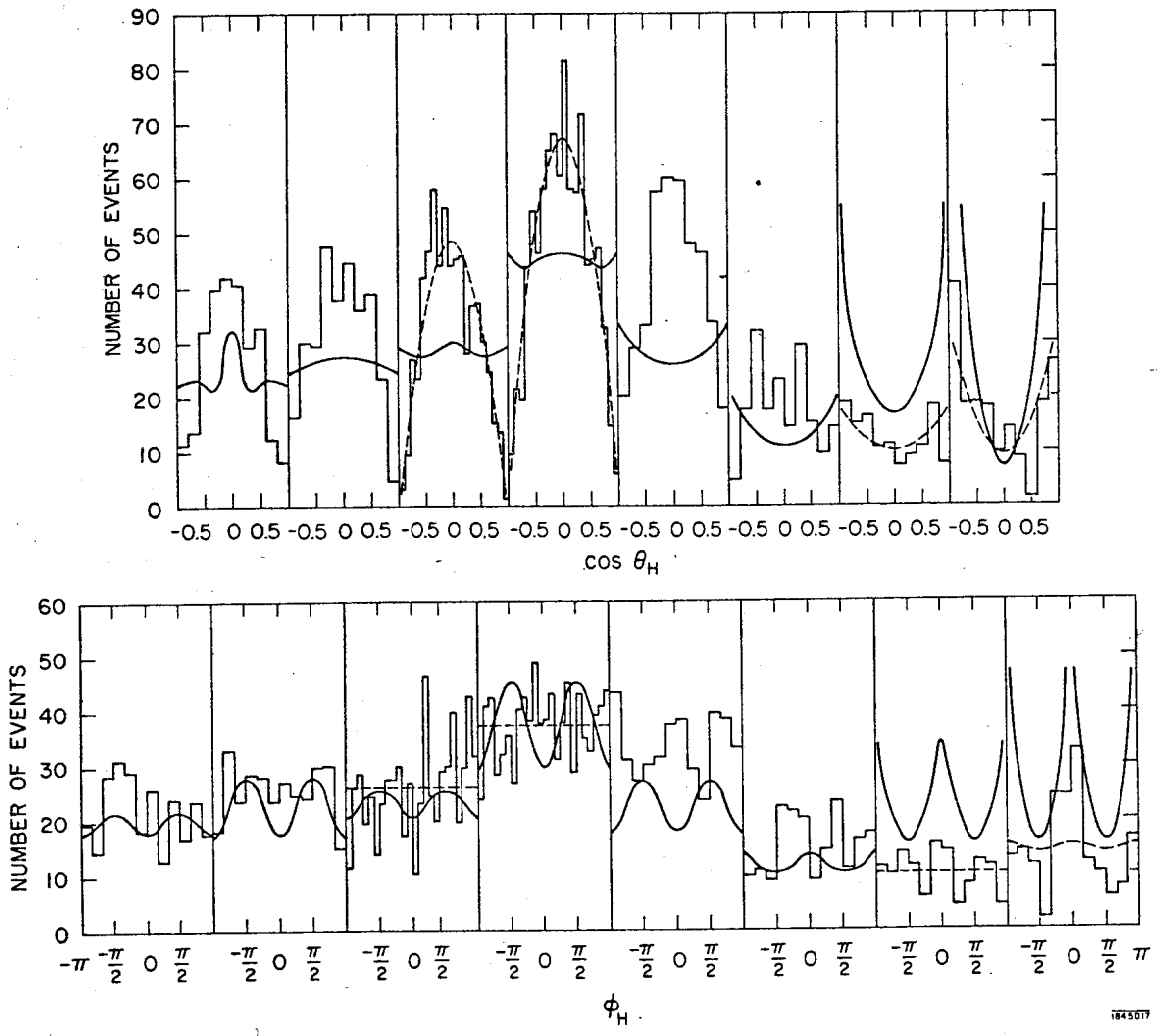

Fig. 9

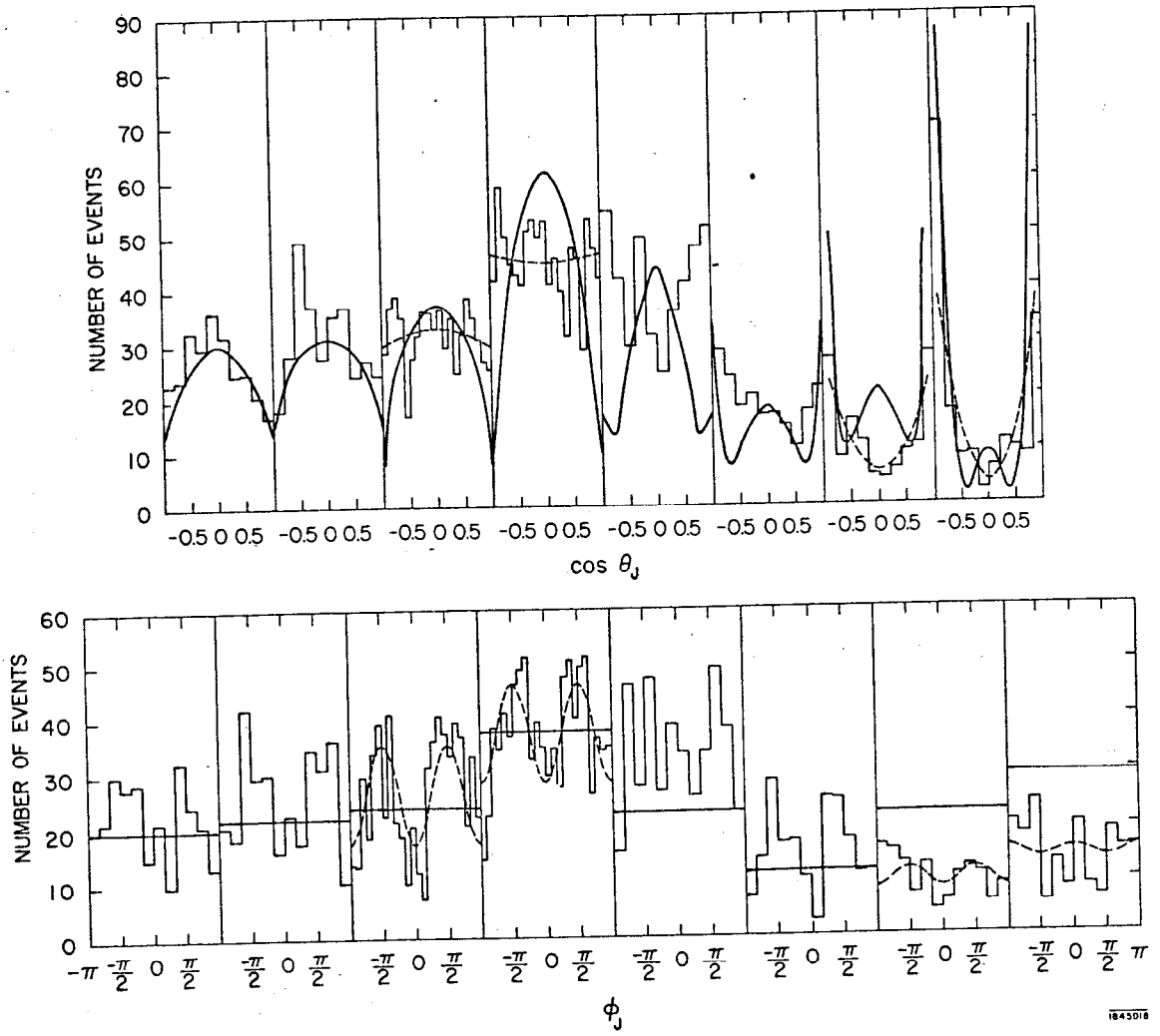

Fig. 10